Geodesic Active Contours Applied to Texture Feature Space

Chen Sagiv[1], Nir A. Sochen[1], and Yehoshua Y. Zeevi[2]

[1] Department of Applied Mathematics
University of Tel Aviv
Ramat-Aviv, Tel-Aviv 69978, Israel
chensagi@post.tau.ac.il, sochen@math.tau.ac.il
[2] Department of Electrical engineering
Technion - Israel Institute of Technology
Technion City, Haifa 32000, Israel
zeevi@ee.technion.ac.il

Abstract. Gabor Analysis is frequently used for texture analysis and segmentation. Once the Gaborian feature space is generated it may be interpreted in various ways for image analysis and segmentation. Image segmentation can also be obtained via the application of "snakes" or active contour mechanism, which is usually used for gray-level images. In this study we apply the active contour method to the Gaborian feature space of images and obtain a method for texture segmentation. We calculate six localized features based on the Gabor transform of the image. These are the mean and variance of the localized frequency,orientation and intensity. This feature space is presented, via the Beltrami framework, as a Riemannian manifold. The stopping term, in the geodesic snakes mechanism, is derived from the metric of the features manifold. Experimental results obtained by application of the scheme to test images are presented.

1 Introduction

Gaborian approach to image processing and analysis has been motivated by biological principles of image representation at the level of the primary visual cortex. The Gabor framework has been extensively used over the last fifteen years for texture analysis and segmentation [15,11,1].

The motivation for using Gabor filters in texture analysis is double fold. First, it appears as though simple cells in the visual cortex can be well modeled by Gabor functions [12,4], and that the Gabor scheme provides a suitable representation for visual information in the combined frequency-position space [14]. Second, the Gabor representation is optimal in the sense of minimizing the joint two-dimensional uncertainty in the combined spatial-frequency space [5].

Once the Gabor feature space of an image is generated, it may be used for texture segmentation. The fundamental question is how to extract the features which enable us to discriminate between textures. Porat and Zeevi have proposed [15] to extract six localized features that can describe textures: the first

M. Kerckhove (Ed.): Scale-Space 2001, LNCS 2106, pp. 344–352, 2001.

two moments of the spatial frequency, orientation of the spatial frequency and intensity information. The six resulting features were used for texture analysis and synthesis.

Segmentation is another important task in image processing. Since the introduction of "snakes" or active contours [6], this method has been extensively used for boundary detection in gray-level images. In this framework an initial contour is deformed towards the boundary of an object to be detected. The evolution equation is derived from minimization of an energy functional, which obtains a minimum for a curve located at the boundary of the object.

The geodesic or geometric active contours model [3,7] offers a different perspective for solving the boundary detection problem; It is based on the observation that the energy minimization problem is equivalent to finding a geodesic curve in a Riemannian space whose metric is derived from the image contents. The geodesic curve can be found via a geometric flow. Utilization of the Osher and Sethian level set numerical algorithm [16] allows automatic handling of changes of topology.

This snakes' model was extended to the vector valued active contours to handle more complex scenery such as color images [17] and multi-texture images. Some recent related work includes the one of Paragios and Deriche [13] who generate the image texture feature space by filtering the image using Gabor filters. Texture information is then expressed using statistical measurements, and segmentation is achieved by application of geodesic snakes to the statistical feature space. Shah [18] developed and applied curve evolution and segmentation algorithms where anisotropic metrics were considered. Lorigo et al [10] used both image intensity and its variance for MRI image segmentation.

It was shown recently that the Gaborian spatial-feature space can be described, via the Beltrami framework, as a 4D Riemannian manifold embedded in R^6 [8]. Based on this approach we aim to generalize the intensity based geodesic active contours method to the Gabor-feature space of images. The stopping term, in the geodesic snakes mechanism, is generalized and derived from the metric of the Gabor spatial-feature manifold. We treat the localized texture features suggested in [15] as a multi-valued image and apply the geodesic snakes mechanism to it.

2 Geodesic Active Contours

In this section we review the geodesic and geometric active contours method in the context of gray-level images [3,7].

Let $\mathbf{C}(\mathbf{q}) : [0,1] \rightarrow R^2$ be a parametrized curve, and let $I : [0,a] \times [0,b] \rightarrow R^+$ be the given image. Let $E(r) : [0,\infty[\rightarrow R^+$ be an inverse edge detector, so that E approaches zero when r approaches infinity. Minimizing the energy functional proposed in the classical snakes is generalized to finding a geodesic curve in a Riemannian space by minimizing:

$$L_R = \int E(|\nabla I(\mathbf{C}(q))|)\,|\mathbf{C}'(q)|dq. \tag{1}$$

The resultant evolution equation is the gradient descent flow:

$$\frac{\partial \mathbf{C}(t)}{\partial t} = E(|\nabla I|)k\mathbf{N} - (\nabla E \cdot \mathbf{N})\ \mathbf{N}, \tag{2}$$

where k denotes curvature.

Defining a function U, such that $\mathbf{C} = ((x,y)|U(x,y) = 0)$, we may use the Osher-Sethian Level-Sets approach [16] and obtain an evolution equation for the embedding function U:

$$\frac{\partial U(t)}{\partial t} = |\nabla U|\mathrm{Div}\left(E(|\nabla I|)\frac{\nabla U}{|\nabla U|}\right). \tag{3}$$

A popular choice for the stopping function $E(|\nabla I|)$ is given by:

$$E(I) = \frac{1}{1+|\nabla I|^2},$$

but other functions have been considered as well.

3 Feature Space and Gabor Transform

The Gabor scheme and Gabor filters have been studied by numerous researchers in the context of image representation, texture segmentation and image retrieval. A Gabor filter centered at the 2D frequency coordinates (U,V) has the general form of:

$$h(x,y) = g(x',y')\exp(2\pi i(Ux+Vy)) \tag{4}$$

where

$$(x',y') = (x\cos(\phi)+y\sin(\phi), -x\sin(\phi)+y\cos(\phi)), \tag{5}$$

the $2D$ Gaussian window is

$$g(x,y) = \frac{1}{2\pi\sigma^2}\exp\left(-\frac{x^2}{2\lambda^2\sigma^2}-\frac{y^2}{2\sigma^2}\right), \tag{6}$$

λ is the aspect ratio between x and y scales, σ is the scale parameter, and the major axis of the Gaussian is oriented at angle ϕ relative to the x-axis and to the modulating sinewave gratings.

The Fourier transform of the Gabor function is, accordingly :

$$H(u,v) = \exp\left(-2\pi^2\sigma^2((u'-U')^2\lambda^2+(v'-V')^2)\right), \tag{7}$$

where, (u',v') are rotated frequency axes and (U',V') are the rotated coordinates of the central frequency. Thus, $H(u,v)$ is a bandpass Gaussian with minor axis oriented at angle ϕ from the u-axis, and the radial center frequency F is defined by : $F = \sqrt{(U^2+V^2)}$, with orientation $\theta = \arctan(V/U)$. Since maximal resolution in orientation is desirable, the filters whose sine gratings are cooriented

with the major axis of the modulating Gaussian are usually considered ($\phi = \theta$ and $\lambda > 1$), and the Gabor filter is reduced to: $h(x, y) = g(x, y) \exp(2\pi i F x)$.

It is possible to generate Gabor-Morlet wavelets from a single mother-Gabor-wavelet by transformations such as: translations, rotations and dilations. We can generate, in this way, a set of filters for a known number of scales, S, and orientations K. We obtain the following filters for a discrete subset of transformations:

$$h_{mn}(x, y) = a^{-m} h(\frac{x'}{a^m}, \frac{y'}{a^m}), \tag{8}$$

where (x', y') are the spatial coordinates rotated by $\frac{\pi n}{K}$ and $m = 0...S - 1$. Alternatively, one can obtain Gabor wavelets by logarithmically distorting the frequency axis [14] or by incorporating multiwindows [20]. In the latter case one obtains a more general scheme wherein subsets of the functions constitute either wavelet sets or Gaborian sets.

The feature space of an image is obtained by the inner product of this set of Gabor filters with the image:

$$W_{mn}(x, y) = R_{mn}(x, y) + iJ_{mn}(x, y) = I(x, y) * h_{mn}(x, y). \tag{9}$$

Next, we follow Porat and Zeevi [15] and extract six localized texture features from the Gabor feature space: dominant localized frequency (denoted MF), variance of the dominant localized frequency (VF), dominant orientation (MT), variance of the dominant orientation (VT), mean of the local intensity (MI) and variance of the localized intensity level (VI). This selection is based on the assumption that the primitives of natural textures are localized frequency components in the form of Gabor elementary functions. Therefore, texture analysis takes the form of inner product or correlation of such primitives with textured images.

The spatial frequencies are determined by the scale parameter a and a base frequency F_0 as: $F_m = F_0 * a^m$, where m is an integer. The dominant localized frequency is given by:

$$MF(x, y) = \frac{\sum_{i=1}^{m} \sum_{i=1}^{n} W_{mn}(x, y) F_m(x, y)}{\sum_{i=1}^{m} \sum_{i=1}^{n} W_{mn}(x, y)} \tag{10}$$

The variance of the localized frequency VF is

$$VF(x, y) = \frac{\sum_{i=1}^{m} |F_m(x, y) - MF(x, y)|}{m} \tag{11}$$

This feature represents the bandwidth of the localized spatial frequency. If it is normalized by the mean localized frequency we obtain a scale invariant feature.

$$VF_{normalized}(x, y) = \frac{VF(x, y)}{MF(x, y)} \tag{12}$$

The mean and variance of the orientation are defined by

$$MT(x, y) = \frac{\sum_{i=1}^{m} \sum_{i=1}^{n} W_{mn}(x, y) T_n(x, y)}{\sum_{i=1}^{m} \sum_{i=1}^{n} W_{mn}(x, y)} \tag{13}$$

$$VT(x,y) = \frac{\sum_{i=1}^{n} |T_n(x,y) - MT(x,y)|}{n} \tag{14}$$

where $T_n = \frac{\pi n}{K}$.

The local mean intensity and its variance are extracted to complete the set of features. If the image contains smooth segments then the gray level information is the only way to separate these regions. The locality of these features is accomplished by averaging the intensity level using a filter equal in size to the Gabor filter used to generate the Gabor-feature-space:

$$MI(x,y) = \frac{\sum_{x,y \in A} I(x,y)}{N}, \tag{15}$$

where A is the set of N pixels belonging to the area defined by the averaging filter window centered at (x,y) and $I(x,y)$ is the intensity image. The variance of the intensity level is given by

$$VI(x,y) = \frac{\sum_{x,y \in A} |I(x,y) - MI(x,y)|}{N} \tag{16}$$

4 Application of Geodesic Snakes to the Localized-Texture-Features-Space

Application of the geodesic snakes mechanism to the localized texture feature space, derived from the Gabor space of images, is achieved by generalizing the inverse edge indicator function E, which attracts in turn the evolving curve towards the boundary in the classical and geodesic snakes schemes. A special feature of our approach is the metric introduced in the localized texture feature space, and used as the building block for the stopping function E in the geodesic active contours scheme.

Sochen et al [19] proposed to view images and image feature space as Riemannian manifolds embedded in a higher dimensional space. For example, a gray scale image is a 2-dimensional Riemannian surface (manifold), with (x,y) as local coordinates, embedded in R^3 with (X,Y,Z) as local coordinates. The embedding map is $(X = x, Y = y, Z = I(x,y))$, and we write it, by abuse of notations, as (x,y,I). When we consider feature spaces of images, e.g. color space, statistical moments space, and the Gaborian space, we may view the image-feature information as a N-dimensional manifold embedded in a $N+M$ dimensional space, where N stands for the number of local parameters needed to index the space of interest and M is the number of feature coordinates. In our case, we may view the localized features image as a 2D manifold with local coordinates (x,y) embedded in a 8D feature space. The embedding map is (x,y,MF,VF,MT,VT,MI,VI).

MF, VF, MT, VT, MI, VI are functions of the local coordinates (x,y) and are the localized texture features, as described in the previous section.

A basic concept in the context of Riemannian manifolds is distance. For example, we take a two-dimensional manifold Σ with local coordinates (σ_1, σ_2).

Since the local coordinates are curvilinear, the distance is calculated using a positive definite symmetric bilinear form called the metric whose components are denoted by $g_{\mu\nu}(\sigma_1, \sigma_2)$: $ds^2 = g_{\mu\nu} d\sigma^\mu d\sigma^\nu$, where we used the Einstein summation convention : elements with identical superscripts and subscripts are summed over. The metric on the image manifold is derived using a procedure known as pullback [19]. The manifold's metric is then used for various geometrical flows. We shortly review the pullback mechanism [19].

Let $X : \Sigma \rightarrow M$ be an embedding of Σ in M, where M is a Riemannian manifold with a metric h_{ij} and Σ is another Riemannian manifold. We can use the knowledge of the metric on M and the map X to construct the metric on Σ. This pullback procedure is as follows:

$$(g_{\mu\nu})_\Sigma(\sigma^1, \sigma^2) = h_{ij}(X(\sigma^1, \sigma^2)) \frac{\partial X^i}{\partial \sigma^\mu} \frac{\partial X^j}{\partial \sigma^\nu}, \tag{17}$$

where we used the Einstein summation convention, $i, j = 1, \ldots, dim(M)$, and σ^1, σ^2 are the local coordinates on the manifold Σ.

If we pull back the metric of a $2D$ image manifold from the Euclidean embedding space (x,y,I) we get:

$$(g_{\mu\nu}(x, y)) = \begin{pmatrix} 1 + I_x^2 & I_x I_y \\ I_x I_y & 1 + I_y^2 \end{pmatrix}. \tag{18}$$

The determinant of $g_{\mu\nu}$ yields the expression : $1 + {I_x}^2 + {I_y}^2$. Thus, we can rewrite the expression for the stopping term E in the geodesic snakes mechanism as follows:

$$E(|\nabla I|) = \frac{1}{1 + |\nabla I|^2} = \frac{1}{\det(g_{\mu\nu})}. \tag{19}$$

The exact geometry of texture feature space is not known. Therefore, for simplicity, we assume it is Euclidean. Moreover, since we have no previous knowledge on the $2D$ feature-manifold metric, we assume that the distances measured on the $2D$ manifold are the same as those measured in the $8D$ embedding space. Thus, we may use the pullback mechanism to obtain the following metric:

$$(g_{\mu\nu}) = \begin{pmatrix} 1 + \sum_i (C_i A_x^i)^2 & \sum_i C_i C_i A_x^i A_y^i \\ \sum_i C_i C_i A_x^i A_y^i & 1 + \sum_i (C_i A_y^i)^2 \end{pmatrix} \tag{20}$$

where $\mathbf{A} = (\mathbf{MF}, \mathbf{VF}, \mathbf{MT}, \mathbf{VT}, \mathbf{MI}, \mathbf{VI})$, C_i are regularization factors which account for the different physical dimensions for each parameter, and i goes over all members of this set.

The metric g derived in this section is strictly used for the purpose of calculating an edge detector. It is used to measure distances on manifolds and its components indicate the rate of change of the manifold given a certain direction. Therefore, the determinant of the metric is used as a positive definite edge indicator: A large value indicates a strong gradient, while a small value indicates where the manifold is almost flat. Thus, it is reasonable to set E to be the inverse of the determinant of $g_{\mu\nu}$.

5 Results and Discussion

In our application of geodesic snakes to textural images, we have used the mechanism offered by Lee [9] to generate the Gabor wavelets for five scales and eight orientations. In the geodesic snakes mechanism U was initiated to be a signed distance function [3]. For simplicity, we have set the values of C_i discussed in section 4 to be 1. Following are the results for a few test im-

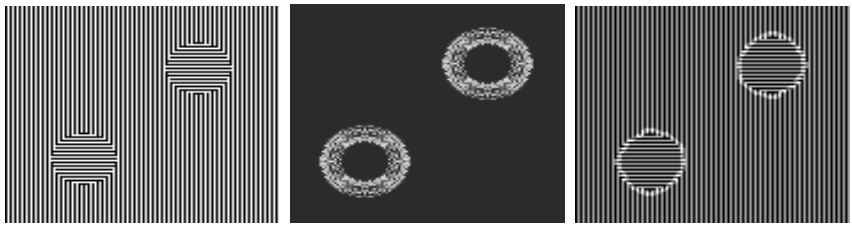

Fig. 1. a. A synthetic image made up of 2D sinewave gratings containing background and object of different orientations (left). b. The stopping function E (middle). c. The resultant boundary(right).

ages. For the complete set of full size images and a demo see the web-page: `http://www-visl.technion.ac.il/scalespace01`.

In the first example (Fig. 1) the test image is a synthesized texture composed of vertical and horizontal lines. Application of the geodesic snakes algorithm results in an accurate boundary. In the second example the test image is composed of two textures which differ in their scale (Fig. 2). The resultant boundary is located at the interior of the circles rather than on their exact boundary. The reason for that might be that since the two textures are quite similar, the change of scale is noted by the Gabor filters only when they are properly located within the internal texture.

Our next example is composed of two different textures taken from the Brodatz album (Fig. 3). Since these textures are characterized by small variations in their dominant scale and orientation the six localized features are submitted to non linear smoothing prior to the generation of the stopping term E which is also in turn smoothed by the same process. The non linear smoothing procedure used is the Beltrami flow as described in [19]. The degree of smoothing was empirically determined to obtain satisfactory results.

We have shown that it is useful to extend the definition of the stopping term E used in the geodesic snakes scheme to features other than intensity gradients. In the original work the six localized features are used as vector components to determine distance between textures [15]. This allows for determining the mean value of these features for each texture. In the proposed segmentation process the localized features are calculated for each pixel and therefore hold a large

Fig. 2. a. A synthetic image made up of 2D sinewave gratings containing background and object of different scales (left). b. The stopping function E (middle). c. The resultant boundary(right).

degree of intra-variation. Thus, if the texture is not homogeneous we may need higher statistical moments such as kurtosis of the localized texture features. Yet, we have shown that this algorithm can be successfully applied to textures that are characterized by a small degree of intra-variation.

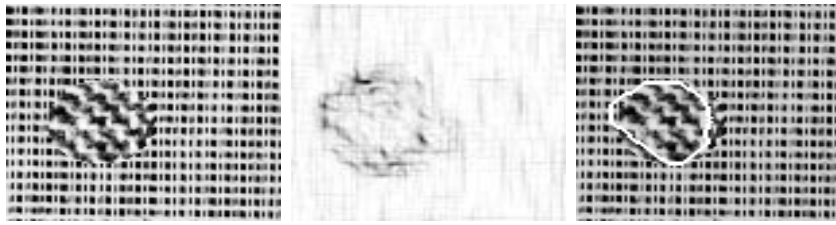

Fig. 3. a. An image comprised of two textures taken from Brodatz album of textures [2] (left). b. The stopping function E (middle). c. The resultant boundary(right).

Acknowledgments: This research has been supported in part by the Israeli Ministry of Science, by the Ollendorff Minerva Center of the Technion, and by the Fund for Promotion of Research at the Technion.

References

1. A.C. Bovik and M. Clark and W.S. Geisler "Multichannel Texture Analysis Using Localized Spatial Filters", *IEEE Transactions on PAMI*, 12(1), 1990, 55-73.
2. P. Brodatz, Textures: A photographic album for Artists and Designers, New York, NY, Dover, 1996.

3. V. Caselles and R. Kimmel and G. Sapiro, "Geodesic Active Contours", *International Journal of Conputer Vision*, 22(1), 1997, 61-97.
4. J.G. Daugman, "Uncertainty relation for resolution in space, spatial frequency, and orientation optimized by two-dimensinal visual cortical filters", *J. Opt. Soc. Amer.* 2(7), 1985, 1160-1169.
5. D. Gabor "Theory of communication"*J. IEEE* , 93, 1946, 429-459.
6. M. Kaas, A. Witkin and D. Terzopoulos, "Snakes : Active Contour Models", *International Journal of Computer Vision*, 1, 1988, 321-331.
7. S. Kichenassamy, A. Kumar, P. Olver, A. Tannenbaum and A. Yezzi, "Gradient Flows and Geometric Active Contour Models",*Proceedings ICCV'95*, Boston, Massachusetts, 1995, 810-815.
8. R. Kimmel, R. Malladi and N. Sochen, "Images as Embedded Maps and Minimal Surfaces: Movies, Color, Texture, and Volumetric Medical Images",*International Journal of Computer Vision*, 39(2), 2000, 111-129.
9. T.S. Lee, "Image Representation using 2D Gabor-Wavelets", *IEEE Transactions on PAMI*, 18(10), 1996, 959-971.
10. L.M. Lorigo, O. Faugeras, W.E.L. Grimson, R. Keriven, R. Kikinis, "Segmentation of Bone in Clinical Knee MRI Using Texture-Based Geodesic Active Contours", *Medical Image Computing and Computer-Assisted Intervention*, 1998, Cambridge, MA, USA.
11. B.S. Manjunath and W.Y. Ma, "Texture features browsing and retrieval of image data", *IEEE Transactions on PAMI*, 18(8), 1996, 837-842.
12. S. Marcelja, "Mathematical description of the response of simple cortical cells", *J. Opt. Soc. Amer.*, 70, 1980, 1297-1300.
13. N. Paragios and R. Deriche, "Geodesic Active Regions for Supervised Texture Segmentation", *Proceedings of International Conference on Computer Vision*, 1999, 22-25.
14. M. Porat and Y.Y. Zeevi, "The generalized Gabor scheme of image representation in biological and machine vision", *IEEE Transactions on PAMI*, 10(4), 1988, 452-468.
15. M. Porat and Y.Y. Zeevi, "Localized texture processing in vision: Analysis and synthesis in the gaborian space", *IEEE Transactions on Biomedical Engineering*, 36(1), 1989, 115-129.
16. S.J. Osher and J.A. Sethian, "Fronts propagating with curvature dependent speed: Algorithms based on Hamilton-Jacobi formulations", *J of Computational Physics*, 79, 1988, 12-49.
17. G. Sapiro, "Vector Valued Active Contours", *Proc. IEEE Conference on Computer Vision and Pattern Recognition*, 680-685, 1996.
18. Jayant Shah, "Riemannian Drums, Anisotropic Curve Evolution and Segmentation",*Proceedings of Scale-Space 1999.*, Eds. Nielsen, P. Johansen, O.F. Olsen, J. Weickert, Springer, 129-140.
19. N. Sochen, R. Kimmel and R. Malladi , "A general framework for low level vision", *IEEE Trans. on Image Processing*, 7, (1998) 310-318.
20. M. Zibulski and Y.Y. Zeevi, "Analysis of multiwindow Gabor-type schemes by frame methods", *Applied and Computational Harmonic Analysis*, 4, 1997, 188-221.